Investigation of the Scanning Tunneling Microscopy Image, the Stacking Pattern and the Bias-voltage Dependent Structural Instability of 2,2'-Bipyridine Molecules Adsorbed on Au(111) in Terms of Electronic Structure Calculations

Youngsun Suh, Sung Soo Park,[†] Jinhee Kang, Yong Gyoo Hwang, D. Jung, Dong Hee Kim,[‡] Kee Hag Lee,[*] and M.-H. Whangbo[§]

Department of Chemistry, Nanoscale Science and Technology Institute, and BK21, Wonkwang University, Iksan 570-749, Korea
[*]E-mail: khlee@wonkwang.ac.kr
[†]CAE Group, Central R&D Institute, Samsung Electro-Mechanics Co., Ltd., Suwon 443-803, Korea
[‡]Department of Chemistry, Kunsan National University, Kunsan 573-701, Korea
[§]Department of Chemistry, North Carolina State University, Raleigh, North Carolina 27695-8204, USA
Received December 5, 2007

A self-assembled monolayer of 2,2'-bipyridine (22BPY) molecules on Au(111) underwent a structural phase transition when the polarity of a bias voltage was switched in scanning tunneling microscopy (STM) experiments. The nature of two bright spots representing each 22BPY molecule on Au(111) in the high-resolution STM images was identified by calculating the partial density plots for a monolayer of 22BPY molecules adsorbed on Au(111) using tight-binding electronic structure calculations. The stacking pattern of the chains of 22BPY molecules on Au(111) was explained by examining the intermolecular interactions between the 22BPY molecules based on first principles electronic structure calculations for a 22BPY dimer, $(22BPY)_2$. The structural instability of the 22BPY molecule arrangement caused by a change in the bias voltage switch was investigated by estimating the adsorbate-surface interaction energy using a point-charge approximation for Au(111).

Key Words : 2,2'-Bipyridine on Au(111), Adsorbate-surface interaction, Scanning tunneling microscopy image interpretation, First principles calculations, Tight-binding band calculations.

Introduction

2,2'-Bipyridine (22BPY) is a typical bidentate chelating agent for transition metal ions, and its derivatives are among the most widely utilized class of ligands in coordination chemistry.[1,2] Metal-22BPY complexes have been investigated for many applications, including photocatalytic systems, electroluminescent devices, solar cells, and DNA repair schemes.[3] 22BPY has two pyridine rings connected via a C2-C2' bond, which has been estimated to have approximately 10% double-bond character.[4] 22BPY can have several conformations, as shown in Scheme 1. In principal, the molecule may assume different conformations when adsorbed on a metal surface. The first conformation is the coplanar *cis*-form (180° angle of rotation) with a dipole moment equal to 3.8D and C_{2v} symmetry. The second conformation is the coplanar trans-conformation (0° angle of rotation) with a zero dipole moment and C_{2h} symmetry for an isolated 22BPY molecule.

Two pyridine rings can be rotated around the C2-C2' axis by an angle between 0° and 180° resulting in a geometry with C_2 symmetry.[5] 22BPY shows a s-trans-planar conformation (Scheme 1b) and has C_{2h} symmetry in the crystalline state.[5] When incorporated into metal complexes, 22BPY functions as a bidentate ligand (chelate effect). In these cases, it exists in a *cis* coplanar conformation (Scheme 1a) and has C_{2v} symmetry. However, lower symmetry conformations must exist between these two extremes (Scheme 1c). In solution, the molecule is in its transoidal-conformation, which is in agreement with quantum chemical calculations.[6]

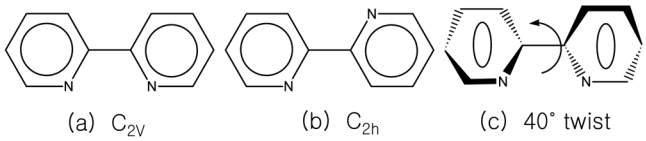

Scheme 1. Possible conformations for 22BPY. (a) *cis*-configuration; (b) trans-configuration; (c) cisoid-(twisted) configuration with a torsion angle of approximately 40°.

The adsorption of 22BPY at the Au(111) solution interface has been examined using cyclic voltammetry, a.c. voltammetry, chronocoulometry, and second-harmonic generation.[7] These results suggest that 22BPY is adsorbed in a flat orientation at the negatively-charged interface with the two aromatic rings parallel to the gold surface. The molecules assume a vertical orientation at the positively-charged surface with the two nitrogen atoms of the coplanar *cis*-conformation (as in Scheme 1a) binding the molecule to the surface.[7]

In electrochemical environments, individual organic molecules at the solid-liquid interface adsorb onto the substrate surface and form a monolayer, which can be imaged by scanning tunneling microscopy (STM) as a function of the

substrate potential.[8-10] The charge on the substrate surface can vary significantly by changing the bias voltage between the substrate and reference electrode inserted in the liquid. A surface charge density of as high as ~0.1 electron per atom can be achieved. A change in surface charge density can affect the stability of a molecular arrangement in an adsorbed monolayer, which can induce a structural phase transition.[11]

For heterocyclic molecules with nitrogen lone pairs, the adsorbate-surface interaction on Au(111) involving the nitrogen lone pair orbitals is strong at high substrate potential.[7] When the surface is negatively charged, 22BPY on Au(111) adopts a flat orientation in which the two aromatic rings of 22BPY are parallel to the Au(111) surface. When the surface is positively charged, 22BPY adopts a vertical orientation in a coplanar *cis* configuration in which the two nitrogen atoms face the metal surface. Lipkowski *et al.*[7] reported that 22BPY shows multi-state adsorption on Au(111). At the negatively charged interface, the molecule assumes a flat orientation with the two aromatic rings parallel to the gold surface. A coplanar *cis*-conformation with both nitrogen atoms coordinated to the substrate surface was suggested at the positively charged interface.[7]

22BPY is adsorbed flat on a negatively charged Au(111) surface maintaining the trans configuration, and vertically at a positively charged surface adopting a coplanar *cis* configuration. Moreover, the flat to vertical orientational transition is gradual and goes through a series of torsional intermediate states.[7] Tao *et al.* reported that the 22BPY molecules orient vertically and form a well-ordered phase on a positively charged Au(111) substrate.[12] STM images of the well-ordered phase were interpreted as the 22BPY molecule adopting a *cis* conformation with the two nitrogen atoms toward the surface.[12]

In STM and in situ surface-enhanced infrared absorption spectroscopy (SEIRAS) study, Noda *et al.* observed orientational and two-dimensional phase transitions in the 22BPY adlayer, which facilitate more dense packing of the molecules at more positive potentials.[13] 22BPY is adsorbed flat at < –0.4V(SCE) and vertically at more positive potentials. The vertically oriented 22BPY molecules adopt a *cis* conformation and coordinate to the surface through the two nitrogen atoms. In association with the flat to vertical orientational transition, the ordered domains in which molecules are stacked into rows like 'rolls of coins' are formed.[13]

From an analysis of their high-resolution STM images, Tao et al. reported that each 22BPY molecule is represented by two bright spots and suggested that these bright spots are associated with the two nitrogen atoms of 22BPY (Figure 1).[14] To a first approximation, the STM image of a sample is well described by the partial electron density plot $\tilde{n}(r_0,e_f)$ of the sample surface.[15-17] These plots were calculated using the extended Hückel tight binding (EHTB) electronic band structure method[18] and have been indispensible in interpreting STM images of many organic and inorganic compounds.

In particular, calculations for hydrocarbons on graphite[16,17]

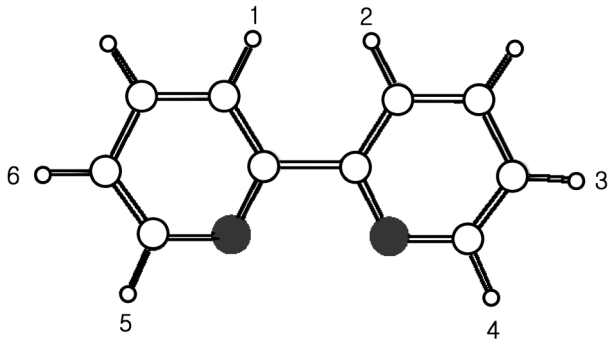

Figure 1. Structure of 2,2'-bipyridine (22BPY). The small and large open circles represent the H and C atoms, respectively, and the filled circles indicate the N atoms.

showed that insulating molecules adsorbed on a metallic substrate can be detected by STM for two reasons: the orbitals of the insulating molecules mix, albeit slightly, into the energy region of the substrate's Fermi level, and the molecules are close to the tip. As the extent of orbital mixing increases, the electron density of the adsorbed molecules in the associated $\rho(r_0, e_f)$ plot increases, so the adsorbed molecules appear as bright spots in the corresponding STM images. It is often the uppermost atoms of the adsorbed molecules closest to the tip that dominate the $\rho(r_0, e_f)$ plot and are observed in the STM images. If the 22BPY molecules adsorbed on Au(111) stand vertically on the surface with the N atoms facing the surface, the two uppermost hydrogen atoms of each 22BPY (*i.e.*, H1 and H2 in Figure 1) would be closest to the tip. Therefore, it is expected that the two spots representing each 22BPY in the STM image would be associated with the two uppermost hydrogen atoms rather than with the two N atoms, which are further away from the tip.

This study examined the nature of two bright spots representing each 22BPY molecule in the high-resolution STM images of 22BPY molecules on a Au(111) surface, the stacking pattern of chains of the 22BPY molecules on Au(111), and the structural instability of the three conformers arrangement of 22BPY caused by a bias voltage switch. In order to achieve this objective, STM images of 22BPY molecules adsorbed on Au(111) were simulated by calculating their partial density plots, examining the binding energy of a 22BPY dimer, $(22BPY)_2$ based on first principles electronic structure calculations, and estimating the surface-charge dependence of the 22BPY-Au(111) interaction with the point-charge approximation for a Au (111) surface.

Partial Density Plots and STM Images

The STM images of 22BPY molecules adsorbed on Au(111) were simulated by calculating the partial density plots $\rho(r_0, e_f)$ based on the EHTB method for a monolayer of 22BPY adsorbed on a slab of Au atoms consisting of three layers of Au atoms parallel to the Au(111) surface. A monolayer of 22BPY molecules was constructed using the

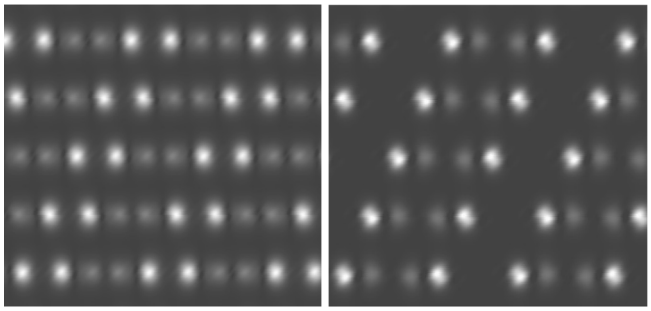

Figure 2. $\rho(r_0,e_f)$ plots calculated for a monolayer of 22BPY molecules adsorbed vertically on a Au(111) surface with r_0 = 3 Å: (a) with the N atoms facing the surface and (b) with the N atoms facing away from the surface. The white circles in (a) refer to the H1 and H2 atom positions, and white circles in (b) the H4 and H5 atom positions. The contrast covers the electron density variations in the 0.0-1.0 × 10^{-8} electrons au^{-3} in (a), and 0.0-4.0 × 10^{-8} electrons au^{-3} in (b).

molecules stacked vertically on Au(111) with an interplanar distance of 3.4 Å (*i.e.*, the van der Waals contact distance between the two carbon atoms). Two vertical arrangements of 22BPY molecules were considered; the N atoms facing the surface (case 1), and N atoms facing away from the surface (case 2). The partial density plots were made on the plane lying 3.0 Å above the upper most atoms of the vertically adsorbed molecules (*i.e.*, r_0 = 3.0 Å).

Figure 2a shows the partial density plot $\rho(r_0,e_f)$ calculated for case 2, *i.e.*, when the H1 and H2 atoms are closest to the tip. The plot shows that each 22BPY molecule is represented by the electron densities of the H1 and H2 atoms. The distance between the two H1 and H2 atoms is approximately 2.1 Å, which is consistent with the distance between the bright spots representing each 22BPY molecule in the high resolution STM images. Figure 2b shows the partial density plot $\rho(r_0,e_f)$ calculated for case 2, *i.e.*, when the H4 and H5 atoms are closest to the tip. The plot shows that each 22BPY molecule is represented by the electron densities of the H4 and H5 atoms with no contribution from the lone pair orbitals of N. The distance between the H4 and H5 atoms of 22BPY is much longer than 2.8 Å (the distance between the two nitrogen atoms is approximately 2.8 Å), which is inconsistent with the distance between the bright spots representing each 22BPY molecule in the high resolution STM images.[14] Consequently, the bright spots in the STM images of the 22BPY molecules adsorbed on Au(111) should be assigned to the H1 and H2 atoms of 22BPY molecules. This means that the 22BPY molecules are adsorbed on Au(111) through interactions with the nitrogen lone pair.

Interaction between 22BPY Molecules

The stacking pattern between 22BPY molecules was analyzed by examining the intermolecular interaction between 22BPY molecules by performing first principles electronic structure calculations for a dimer, $(22BPY)_2$, in which the two molecules are arranged parallel to each other,

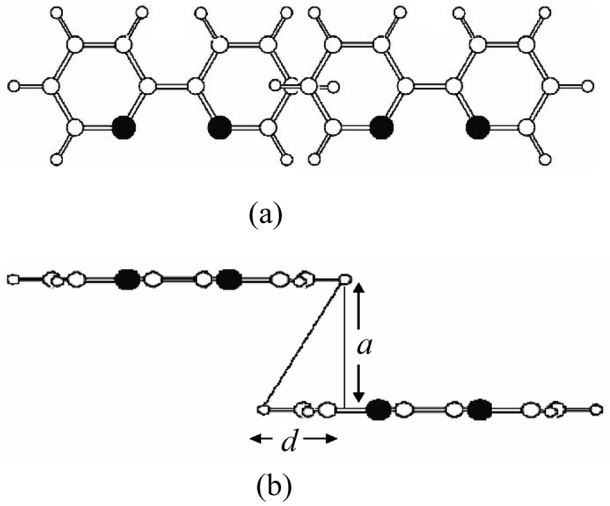

Figure 3. Arrangement of two 22BPY molecules in a dimer $(22BPY)_2$, where *d* is the overlap distance between the two monomers, and *a* is the interplanar distance between the two monomers.

as shown in Figure 3. The relative positions of the two 22BPY molecules in this dimer were determined using the two geometrical parameters *d* and *a*. Here, *a* is the intermolecular distance, and *d* is the extent of overlap between two 22BPY molecules in the top projection view of the dimer. *d* = 0 signifies that the nearest terminal H atoms of the

Table 1. Dimerization energies ΔE (in kcal/mol) of the dimer $(22BPY)_2$ at the local minimum-energy structures under the constraint that the monomers are parallel to each other

a (Å)	d (Å)	ΔE (kcal/mol)
0.8	−2	3908.5
2		3908.5
1.6	0	914.6
4		466.1
2	−3	242.1
3		242.1
11		0.0
2.4	−3	78.6
3		78.5
11		−0.1
2.8	−3	22.7
3		22.6
10		−0.2
3.2	−3	6.1
3		6.0
10		−0.2
3.6	−3	1.8
3		1.8
9		−0.2
4	9	−0.2
4.4	8	−0.2
4.8	2	0.7
8		−0.1
5.2	9	−0.1

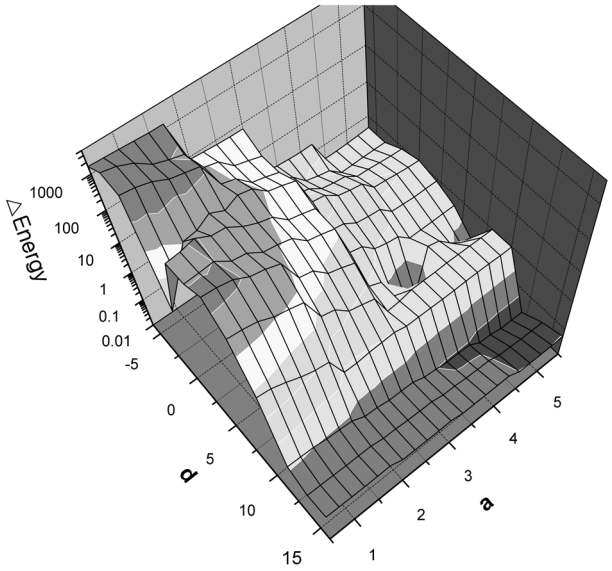

Figure 4. Three-dimensional surface plot of the binding energy ΔE (in kcal/mol) of $(22BPY)_2$ as a function of the gemetrical parameters *d* and *a* (in Å).

two 22BPY molecules just touch in the top projection view, while a negative *d* value indicates that the 22BPY molecules overlap in the top projection view of $(22BPY)_2$. For the electronic structure calculations, the hybrid density functional method was employed at the level of B3LYP/6-311G(d,p) implemented in Gaussian98 code.[19] The structure of 22BPY was kept constant at the structure optimized with the same level of calculations.

The dimerization energy of $(22BPY)_2$, ΔE, which is defined as the energy of the dimer minus twice the energy of the monomer, was calculated as a function of the geometrical parameters *d* and *a*. Table 1 summarizes the computational results for $(22BPY)_2$. Figure 4 shows the essential trends in the calculated dimerization energies as a three-dimensional surface plot. As a function of *a* and *d*, the minimum energy surface of Figure 4 is when the distance between the nearest atoms of two monomers is beyond the van der Waals distance.

Table 1 shows the dimerization energies, ΔE, calculated for the local minimum-energy structures of $(22BPY)_2$, obtained under the constraint that the 22BPY monomers are parallel to each other. Note that in the region of a = 2.0-3.60 Å, there are two minimum-energy structures with differing degrees of overlap between two 22BPY molecules, *i.e.*, one with overlap ($d < 0$) and the other without ($d > 0$). In the region of a = 2.0-3.60 Å, the dimers are with overlap ($d < 0$) of 3 Å (see Figure 3). In the a =2.0 over and d = 8.0 Å region, the dimers have no overlap ($d > 0$) and the dimerization energy ΔE has a negative value. Only when the intermolecular spacing is close to the van der Waals sum of two carbon atoms (*i.e.*, 3.4 Å), the two local minimum-energy structures show comparable stability (Table 1).

Full geometry optimizations for $(22BPY)_2$ in the regions of the low-energy structures lead to six local minimum energy structures with a negative ΔE (*i.e.*, the dimer formation is energetically favorable), as shown in Figure 5a-f. The two most stable structures of $(22BPY)_2$ have C-H···N hydrogen bonds between the two monomers. The remaining four dimer structures originate from interplanar van der Waals interactions and have C-H···H-C hydrogen bonds between the two monomers. The three most stable structures show rotation via around the N-C-C-N single bond at each 22BPY monomer. Optimized and twisted 22BPY dimers show an extent of rotation of approximately 40° The surface in Figure 4 is a flat area in the range of a = 2.0-5.2 Å, and above d = 8 Å. It was assumed that the flat area is consistent with the observation that two kinds of kinks occur in the STM images of 22BPY molecules on Au(111). One sudden translation of a section of a chain in a direction perpendicular to the chain by approximately 2 Å can occur without changing the orientation of the chain with respect to the underlying Au(111) lattice direction. The other translation is the sudden bending of a chain by 120°, which allows the chain to follow an equivalent direction on the Au(111) lattice. These results are similar to those reported for 1,10'-phenanthroline.[20,21]

Therefore, the stacking of 22BPY molecules on Au(111) observed in the STM images should be described in terms of the interactions between the nitrogen lone pair and the gold atom as well as the interplanar van der Waals interactions.[14]

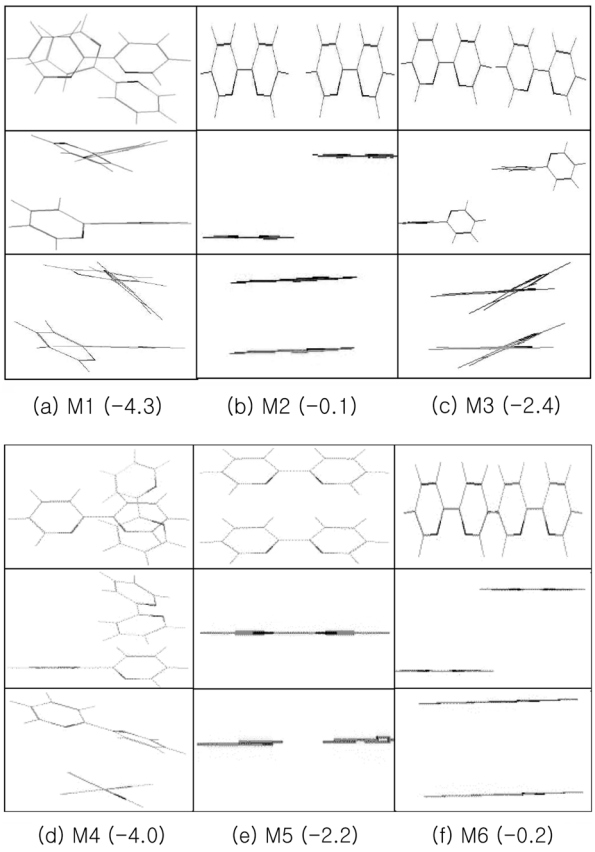

Figure 5. Local minimum-energy structures of $(22BPY)_2$ optimized without constraints at the level of B3LYP/6-311G(d,p). The numbers in parentheses refer to the binding energy (kcal/mol) of the dimer.

Substrate-adsorbate Interaction in Terms of the Point-charge Approximation

Three 22BPY conformers were considered, which are shown in Scheme 1: (a) *cis*-configuration; (b) *trans*-configuration; and (c) cisoid-(twisted) configuration with a torsion angle of approximately 40°. In order to examine how the stability of the monolayer structure of each 22BPY conformer on Au(111) might be affected by a change in bias voltage, it is necessary to estimate the dependence of each 22BPY conformer-Au(111) interaction on the charge of the Au(111) surface induced by the bias voltage. The effect of charge on Au(111) was examined by representing the Au(111) surface by a single sheet of 25 point charges δ located at the 5×5 Au positions on the Au(111) surface (Figure 6) and then performing first principles electronic structure calculations using the B3LYP hybrid method for a 22BPY molecule and the model surface. As shown in Figure 6.1-6.3, three kinds of arrangements were considered between each 22BPY conformer and the model surface with δ = +0.05 and 0.05. Similar results were obtained for the other δ values examined. Therefore, in the following, only those based on δ = +0.05 and 0.05 are discussed. The 22BPY-Au(111) interaction energy, ΔE_s was calculated as a function of the distance *r* between 22BPY and the model surface, where the distance *r* is given from the surface to the closest atoms of 22BPY in each case of the three conformers of 22BPY.

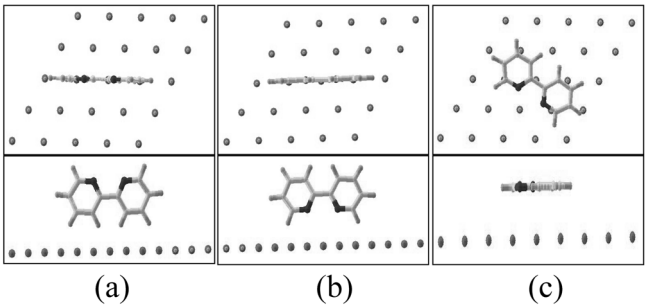

Figure 6.1. Vertical and parallel arrangements of a 22BPY *cis* configuration on a model surface made up of point charges located on the 5×5 mesh points.

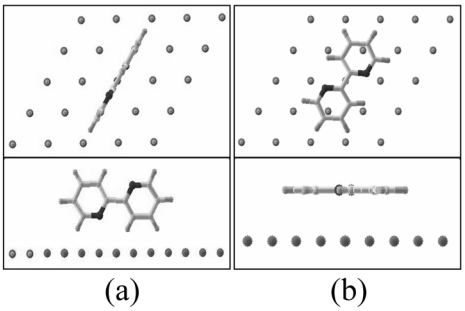

Figure 6.2. Vertical and parallel arrangements of a 22BPY trans configuration on a model surface made up of point charges located on the 5×5 mesh points.

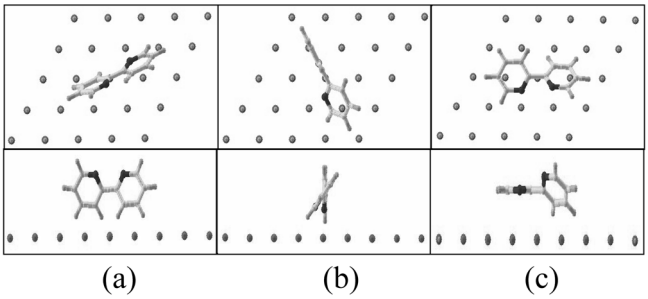

Figure 6.3. Vertical and parallel arrangements of a 22BPY cisoid-(twisted) conformation with a torsion angle of approximately 40° on a model surface made up of point charges located on the 5×5 mesh points.

Figures 7.1-7.3 summarize the calculation results where the interaction energy ΔE_s refers to the energy of a 22BPY molecule interacting with the model surface system minus that of an isolated 22BPY molecule and isolated model surface. The adsorption becomes energetically favorable with decreasing ΔE_s. When the *cis* configuration is perpendicular to the Au(111) surface with the N atoms facing away from the surface, a negative surface charge is more favorable for adsorption than a positive surface charge (Figure 7.1a).

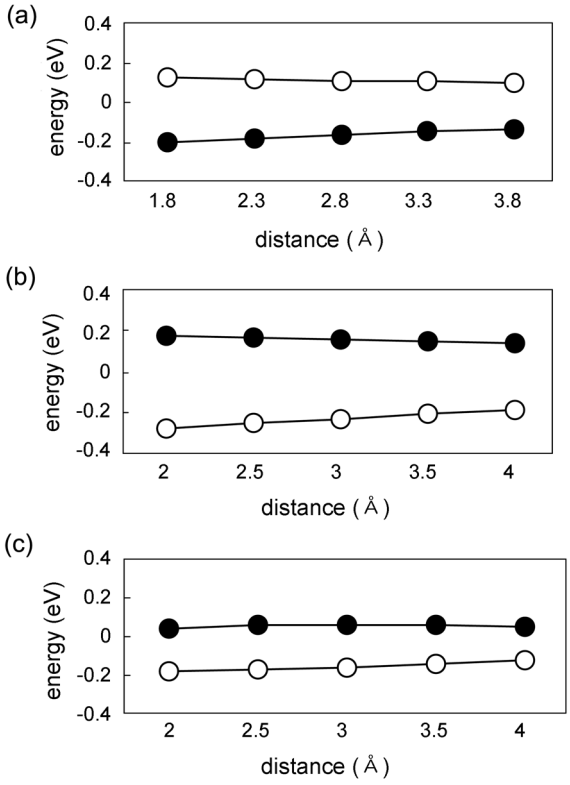

Figure 7.1. 22BPY-Au(111) interaction energy ΔE_s calculated as a function of the distance between the model surface of point charges δ and the closest atoms of the 22BPY *cis* configuration to the surface: (a) a 22BPY *cis* configuration is perpendicular with the N atoms facing away from the surface, (b) a 22BPY *cis* configuration is perpendicular with the N atoms facing the surface, and (c) 22BPY *cis* configuration lies flat and parallel to the surface. The ΔE_s values for δ = 0.05 are represented by filled circles, and those for δ = +0.05 are indicated by empty circles.

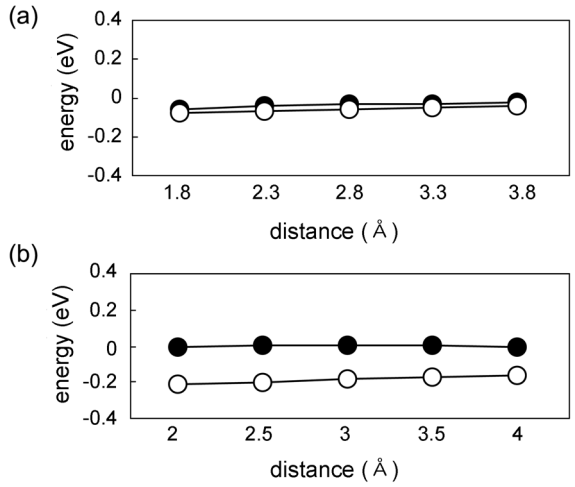

Figure 7.2. 22BPY-Au(111) interaction energy ΔE_s calculated as a function of the distance between the model surface of point charges δ and the closest atoms of the 22BPY trans configuration to the surface: (a) the 22BPY trans configuration is perpendicular with the N atoms facing away from the surface, (b) the 22BPY trans configuration is perpendicular with the N atoms facing the surface, and (c) 22BPY trans configuration lies flat and parallel to the surface. The ΔE_s values for δ = 0.05 are represented by filled circles, and those for δ = +0.05 are indicated by empty circles.

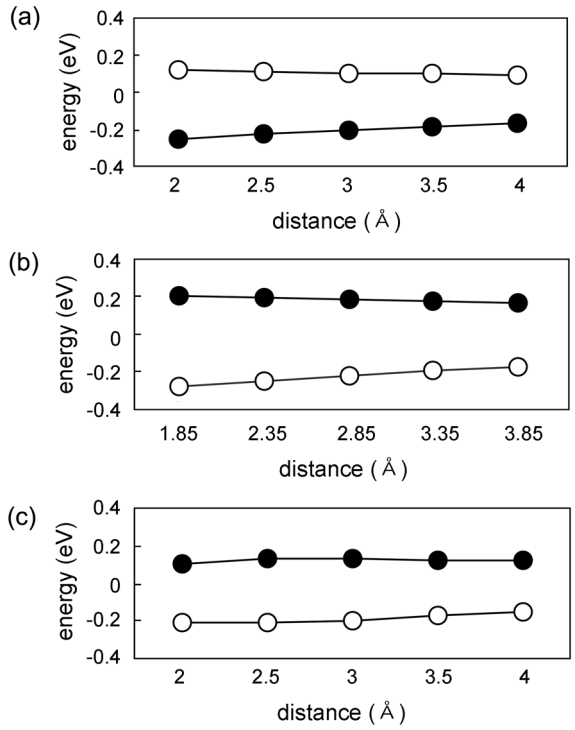

Figure 7.3. 22BPY-Au(111) interaction energy ΔE_s calculated as a function of the distance between the model surface of point charges δ and the closest atoms of 22BPY cisoid-(twisted) conformation with a torsion angle of approximately 40° to the surface: (a) a 22BPY cisoid conformation is perpendicular with the N atoms facing away from the surface, (b) a 22BPY cisoid conformation is perpendicular with the N atoms facing the surface, and (c) 22BPY cisoid conformation lies flat and parallel to the surface. The ΔE_s values for δ = 0.05 are represented by filled circles, and those for δ = +0.05 by empty circles.

When a *cis* configuration is perpendicular to the Au(111) surface with the N atoms facing the surface, a positive surface charge is more favorable for adsorption than a negative surface charge (Figure 7.1b). A positive surface charge is more favorable than the negative surface charge for the flat arrangement of a *cis* configuration (Figure 7.1c). Regardless of the sign of the surface charge, when a trans configuration is perpendicular to the Au(111) surface, it has similar ΔE_s value, in which the gap to error can be ignored (Figure 7.2a). A positive surface charge is more favorable than a negative surface charge for the flat arrangement of a trans configuration (Figure 7.2b). When a cisoid-(twisted) configuration is perpendicular to the Au(111) surface with the N atoms facing away the surface, a negative surface charge is more favorable for adsorption than a positive surface charge (Figure 7.3a). When a cisoid-(twisted) configuration for 22BPY is perpendicular to the Au(111) surface with the N atoms facing the surface, a positive surface charge is more favorable for adsorption than a negative surface charge (Figure 7.3b). Therefore, the cisoid-(twisted) conformation of 22BPY adsorbed on Au(111) at a positively charged surface can be justified energetically. The flat arrangement of the cisoid-(twisted) configuration is more favorable for adsorption on the Au(111) at a positive surface charge than at a negative surface charge (Figure 7.3c). It is clear from the model calculations that the stability of 22BPY adsorption on Au(111) depends on the charge of the Au(111) surface.

This result is consistent with experimental observation[12,14] in which a self-assembled monolayer of 2,2'-bipyridine (22BPY) molecules on Au(111) undergoes a structural phase transition when the bias voltage is switched in STM experiments.

Concluding Remarks

The partial density plots show that the bright spots of the high resolution STM images of 22BPY on Au(111) surface correspond to the hydrogen atoms, H1 and H2, of 22BPY, which means that in a monolyer of 22BPY molecules adsorbed on Au(111), the molecules stand vertically with their nitrogen lone pairs interacting with the surface. The calculated binding energies of $(22BPY)_2$ can explain the "slipping" in the chains of 22BPY molecules observed in the high-resolution STM images of 22BPY molecules on Au(111). The 22BPY-Au(111) interaction energies indicate that the chain structures of the 22BPY molecules in the monolayer on Au(111) can become destabilized when the bias voltage is switched from a positive to a negative value because a switch in bias voltage induces a reversal of the polarity of the surface charge. These results are consistent with the results reported in the literature in that 22BPY adsorbs perpendicular to the positively-charged on the gold surface.[12-14,22-24] The molecule assumes a *cis*-configuration with nitrogen atoms pointing towards the surface.

Acknowledgement. This work was supported by Wonkwang University in 2005.

References

1. Balzani, V.; Bolletta, F.; Gandolfi, M. T.; Maestri, M. *Top. Curr. Chem*. **1978**, *75*, 1.
2. Summers, L. A In *Advances in Heterocyclic Chemistry*; Katritzky, A. R., Ed.; Academic Press: Orlando, 1984; vol. 35, p 281.
3. Dandliker, P. J.; Holmlin, R. E.; Barton, J. K. *Science* **1997**, *275*, 1465.
4. Merritt, L. L.; Schroeder, E. D. *Acta Crystallogr.* **1965**, *195*, 801.
5. Merritt, L. L.; Schroeder, E. D. *Acta Crystallogr.* **1956**, *9*, 1981.
6. Jaime, C.; Font, J. *J. Mol. Stuct*. **1989**, *195*, 1420.
7. Yang, D.; Bizzotto, D.; Lipkowski, J.; Pettinger, B.; Mirwald, S. *J. Phys. Chem*. **1994**, *98*, 7083.
8. (a) Chiang, S. *Chem. Rev.* **1997**, *97*, 1083. (b) Frommer, J. *Angew. Chem. Int. Ed. Engl*. **1992**, *31*, 1298. (c) Gewirth, A. A.; Nice, B. K. *Chem. Rev.* **1997**, *97*, 1129. (d) Noh, J.; Park, H.; Jeong, Y.; Kwon, S. *Bull. Korean Chem. Soc.* **2006**, *27*, 81.
9. (a) Liu, H.-Y.; Fan, F.-R. F.; Lin, C. W.; Bard, A. J. *J. Am. Chem. Soc*. **1986**, *108*, 3838. (b) Sonnenfeld, R.; Hansma, P. K. *Science* **1986**, *232*, 211.
10. Tao, N. J. *Potential Controlled Ordering in Organic Monolayers at Electrode-Electrolyte Interfaces in Imaging of Surfaces and Interfaces* (Frontiers of Electrochemistry, Vol. 5); Lipkowski, J., Ross, P. N., Eds.; Wiley-VCH: New York, 1999.
11. *Adsorption of Molecules at Metal Electrodes*; Lipkowski, J., Ross, P. N., Eds.; VCH: New York, 1992.
12. Cunha, F.; Tao, N. J. *Phys. Rev. Lett*. **1995**, *75*, 2376.
13. Noda, H.; Minoha, T.; Wan, L.-J.; Osawa, M. *J. Electroanalyt. Chem*. **2000**, *48*, 62.
14. Dretschkow, Th.; Lampner, D.; Wandlowski, Th. *J. Electroanalyt. Chem.* **1998**, *458*, 121.
15. Tersoff, J.; Hamman, D. R. *Phys. Rev. B* **1985**, *31*, 805.
16. (a) Liang, W.; Whangbo, M.-H.; Wawkuschewski, A.; Cantow, H.-J.; Magonov, S. *Adv. Mater*. **1993**, *5*, 817. (b) Wawkuschewski, A.; Cantow, H.-J.; Magonov, S.; Möller, M.; Liang, W.; Whangbo, M.-H. *Adv. Mater.* **1993**, *5*, 821.
17. (a) Magonov, S. N.; Whangbo, M.-H. *Adv. Mater.* **1994**, *6*, 355. (b) Magonov, S. N.; Whangbo, M.-H. *Surface Analysis with STM and AFM*; VCH: 1996. (c) Park, S. S.; Lee, J.; Lee, W. R.; Lee, K. H. *Bull. Korean Chem. Soc.* **2007**, *28*, 81.
18. Whangbo, M.-H.; Hoffmann, R. *J. Am. Chem. Soc*. **1978**, *100*, 6093.
19. Frisch, M. J.; Trucks, G. W.; Schlegel, H. B.; Gill, P. M. W.; Johnson, B. G.; Robb, M. A.; Cheeseman, J. R.; Keith, T.; Petersson, G. A.; Montgomery, J. A.; Raghavachari, K.; Al-Laham, M. A.; Zakrzewski, V. G.; Ortiz, J. V.; Foresman, J. B.; Cioslowski, J.; Stefanov, B. B.; Nanayakkara, A.; Challacombe, M.; Peng, C. Y.; Ayala, P. Y.; Chen, W.; Wong, M. W.; Andres, J. L.; Replogle, E. S.; Gomperts, R.; Martin, R. L.; Fox, D. J.; Binkley, J. S.; Defrees, D. J.; Baker, J.; Stewart, J. P.; Head-Gordon, M.; Gonzalez, C.; Pople, J. A. *Gaussian 98*, Revision A.7; Gaussian, Inc.: Pittsburgh, PA, 1998.
20. Cunha, F.; Jin, Q.; Tao, N. J.; Li, C. Z. *Suf. Sci.* **1997**, *389*, 19.
21. Lee, K. H.; Suh, Y.; Lee, C.; Hwang, Y. G.; Koo, H.-J.; Whangbo, M.-H. *J. Phys. Chem. B* **2005**, *109*, 15322.
22. Cunaa, F.; Tao, N. J.; Wang, X. W.; Jin, Q.; Duong, B.; D'Agnese, J. *Langmuir* **1996**, *12*, 6410.
23. Hoon-Khosla, M.; Fawcett, W. R.; Goddard, J. D.; Tian, W.-Q.; Lipkowski, J. *Langmuir* **2000**, *16*, 2356.
24. Dretschkow, T. h.; Wandlowski, T. h. *J. Electroanal. Chem*. **2000**, *467*, 207.
25. Brolo, A. G.; Jiang, Z.; Irish, D. E. *J. Electroanal. Chem*. **2003**, *547*, 163.